engineering proceedings

MDPI

Proceeding Paper

Reliability Analysis of Capstan Drives for Industrial Implementation †

Federico Alonso [1,2,*], Giuliana Brizuela [1,2], Shu-Hao Liang [2] and Marnel Altius [2]

[1] Faculty of Engineering, Universidad Politécnica Taiwán-Paraguay (UPTP), Asunción 001014, Paraguay; giuliana.brizuela@uptp.edu.py
[2] Department of Mechanical Engineering, National Taiwan University of Science and Technology (NTUST), Taipei 106335, Taiwan; shuhaoliang@mail.ntust.edu.tw (S.-H.L.); d11251801@mail.ntust.edu.tw (M.A.)
* Correspondence: federico.alonso@uptp.edu.py
† Presented at the 6th International Conference on Electronic Communications, Internet of Things and Big Data (ICEIB 2026), New Taipei, Taiwan, 24–26 April 2026.

Abstract

Capstan drives offer near-zero backlash, smooth torque transmission, and inherent compliance, making them attractive for precision industrial and robotic applications. However, concerns remain regarding rope slip, elastic deformation, and load-dependent behavior. This study designed and fabricated a capstan transmission using 3D printing and integrated it with a Dynamixel PM42-010-S260-R actuator. Reliability was tested through endurance runs totaling 54,000 cycles with a 1 mm steel wire rope. One rope failed at 14,000 cycles, while two others completed 20,000 cycles each without critical failure. Weibull analysis estimated a characteristic life of 31,560 cycles, supporting the feasibility of capstan drives for industrial use.

Keywords: capstan; slip; robotics; reliability; backlash; gear transmission

1. Introduction

Power transmission systems are vital in industrial machinery and robotic platforms, where precision, efficiency, and reliability define overall performance. Gear-based reducers are widely used due to their high stiffness and well-established design methods. However, they exhibit limitations in precision applications, including backlash, wear-induced positioning errors, and high contact stiffness, which can degrade control performance and excite structural vibrations, especially in dynamic systems such as robotic joints.

Capstan drives offer a promising alternative by transmitting torque through a rope wound around a drum [1–3], enabling near-zero backlash, inherent compliance, and smooth force transmission. These advantages have driven their adoption in cable-driven and legged robotic systems [4–7]. However, their friction-based operation introduces distinct failure modes, such as slip, rope fatigue, and tension loss [8], which remain less understood from a reliability perspective.

By evaluating the reliability of capstan drives as alternatives to gear reducers, such limitations can be addressed. A capstan transmission was designed, fabricated using fused deposition modeling with polyethylene terephthalate glycol-modified (PETG), and tested under identical conditions with a Dynamixel PM42 actuator. Reliability is assessed using transmission error metrics, failure mode and effects analysis [9], and Weibull statistical analysis [10] to provide a structured framework for industrial feasibility.

Reliability in mechanical transmissions is estimated using Weibull statistical models, which distinguish early-life, random, and wear-out failure regimes. For capstan drives

Check for updates

Academic Editors: Teen-Hang Meen, Shu-Han Liao and Cheng-Fu Yang

Published: 17 November 2026

Copyright: © 2026 by the authors. Licensee MDPI, Basel, Switzerland. This article is an open access article distributed under the terms and conditions of the Creative Commons Attribution (CC BY) license.

specifically, the governing failure mechanism is loss of traction between rope and drum, described by the Euler-Eytelwein relation $T_1 = T_2 e^{(\mu\theta)}$, where T_1 and T_2 are the tight-side and slack-side rope tensions, μ is the friction coefficient, and θ is the wrap angle; progressive fretting wear reduces effective friction and pretension until macroscopic slip occurs [3]. Transmission error is adopted as the primary degradation metric, with failure thresholds defined following IEC 60812 and ISO 9283 [9,11].

2. Materials and Methods

The experimental platform comprises a capstan drive testing bench, adapted from previously reported open-source capstan test platforms [5,12]. The capstan drive transmission was fabricated using PETG filament through 3D printing and equipped with a 1 mm steel wire rope. It was driven by a Dynamixel PM42-010-S260-R actuator (ROBOTIS, Seoul, Republic of Korea), which was interfaced with a host computer through a USB to RS485 converter. For angular position measurement, an AS5600 magnetic encoder was incorporated and connected to an ESP32 microcontroller, ensuring accurate monitoring of system performance (Table 1).

Table 1. Key interface for Dynamixel actuators.

Parameter	Value
Actuator	Dynamixel PM42-010-S260-R
Communication	RS485 half-duplex
Baud rate	9600 bps
Interface	USB to RS485 converter (Future Technology Devices International)
Data acquisition	MATLAB R2025a (MathWorks, Natick, MA, USA) with Dynamixel software development kit
Rope material	1 mm steel wire rope
Load application	Dead load (fixed hanging weight)
Gear ratio (capstan)	6.5:1
Rated torque	1 N·m
Motion profile	Continuous back-and-forth rotation (0° to 100°)
AS5600	12-bit magnetic rotary encoder (4096 steps/rev)

The drive system components, including the drums, stand, and connectors, were designed using SolidWorks 2024 computer-aided design software (Dassault Systèmes, Waltham, MA, USA) and fabricated using fused deposition modeling [13]. Initially, polylactic acid was employed for the prototypes. The stand and output gear demonstrated sufficient structural integrity during assembly and initial loading, whereas the input gear experienced catastrophic mechanical failure during assembly and initial loading phases. Consequently, PETG was selected due to its superior toughness [14]. The capstan drive was designed with a 6.5:1 transmission ratio, determined by the drum diameter relationship between the input and output shafts. The diameters of the input and output drums are 21 mm (without 0.5 mm groove) and 126 mm, and with a 0.5 mm space between them for clearance (Figures 1–3).

To ensure experimental repeatability, a pretensioning protocol was implemented. The tension (T) of the 1 mm steel wire rope was verified using the transverse deflection method. A known perpendicular force (F) was applied at the midpoint of a free cable span (L), and the resulting deflection (δ) was measured to calculate the tension:

$$T = \frac{F \cdot L}{4 \cdot \delta} \quad (1)$$

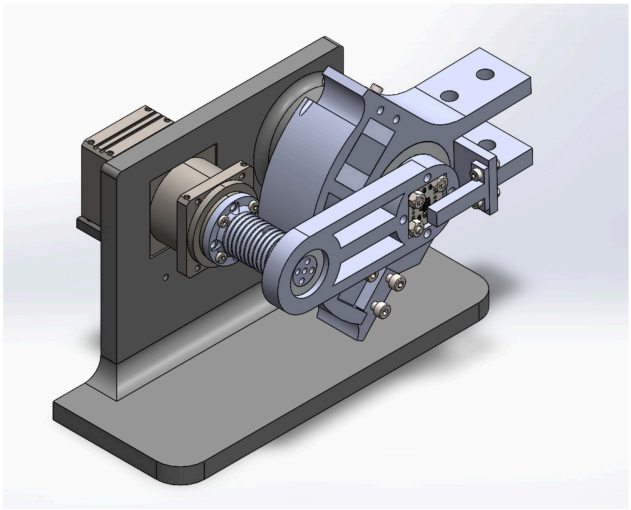

Figure 1. CAD assembly of the 6.5:1 capstan drive transmission, designed in SolidWorks based on the open-source design by Musa [12].

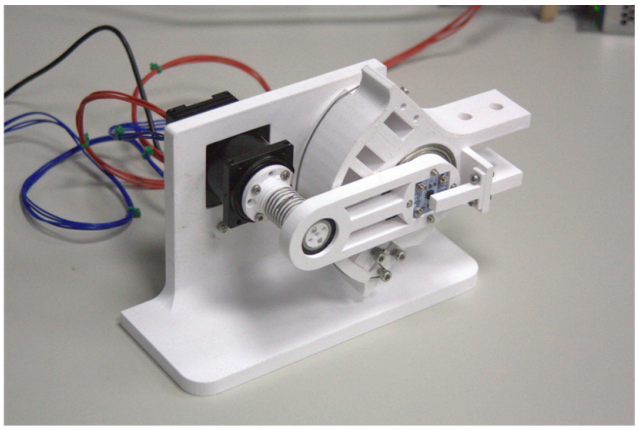

Figure 2. Assembled capstan drive prototype mounted on the experimental test bench.

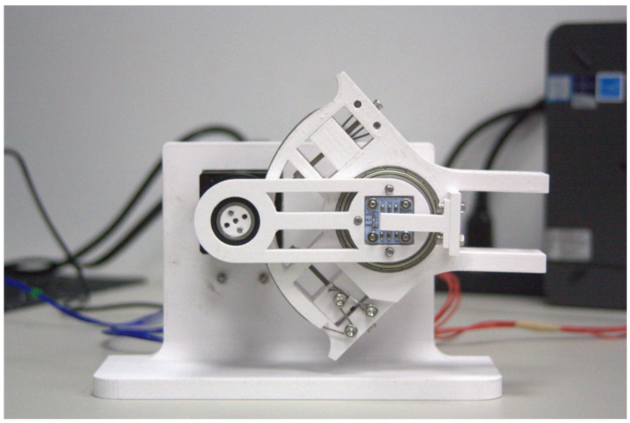

Figure 3. Front view of capstan drive test bench.

The reliability of the capstan drive was evaluated through four tests: baseline characterization, load response, creep, and an accelerated life (endurance) test. The baseline test was conducted to establish reference performance, the load response assessed behavior under varying torque, and the creep test evaluated time-dependent deformation under

sustained load. The endurance test consisted of continuous bidirectional cycles from 0° to 100° at constant speed under nominal load, with the motion range limited to avoid reaching mechanical limits even in the presence of slip. The failure modes and severity thresholds used to classify events in all tests are defined in Table 2.

Table 2. Definition of critical failure modes and structural integrity thresholds.

Severity	Trigger	Threshold
Critical	Rope fracture/structural failure	Any visible break or permanent deformation
Critical	Catastrophic slip/overcurrent	Transmission error (TE) > 15° or current exceeds rated limit
Intermediate	Positional drift	Mean TE > ±3° over 10 cycles
Intermediate	Current increase/repeatable slip	>20% above baseline or ≥3 slips in 10 cycles
Minimal	Positional variation/current drift	±1° from baseline or 5–10% current increase
Minimal	Single slip/surface change	One isolated slip or visible wear without damage

The endurance data were analyzed using a one-parameter Weibull model with right-censored data [15]. A shape parameter of $\beta = 2.0$ was assumed, which is characteristic of progressive wear-out in steel wire rope fatigue. A single capstan drive unit underwent $n = 3$ endurance runs at 55% rated load; the rope was re-tensioned between runs following the protocol and replaced after failure. Runs that ended without a critical failure were treated as suspensions (right-censored). The characteristic life η was estimated by maximum likelihood (Equation (2)), its one-sided lower confidence bound η_L at confidence level C was obtained from the chi-squared distribution (Equation (3)), and the mean time to failure (MTTF) followed from Equation (4).

$$\eta = \left(\frac{\sum_{i=1}^{n} t_i^{\beta}}{r} \right)^{1/\beta} \tag{2}$$

$$\eta_L = \left(\frac{2\sum_{i=1}^{n} t_i^{\beta}}{\chi^2_{C,2r}} \right)^{1/\beta} \tag{3}$$

$$MTTF = \eta \cdot \Gamma\left(1 + 1/\beta\right) \tag{4}$$

Here, t_i is the number of cycles accumulated in run i (to failure or suspension), r is the number of critical failures, $\chi^2_{C,2r}$ is the chi-squared quantile at confidence C with $2r$ degrees of freedom, Γ denotes the Gamma function, and $\Gamma(1.5) = \sqrt{\pi}/2 \approx 0.8862$ for $\beta = 2.0$, representing the expected value scaling factor of the Weibull distribution. A confidence level of 90% was selected following standard practice for accelerated life testing with small test run counts ($n = 3$), consistent with reliability assessment guidelines for mechanical systems [10].

3. Results

The baseline test was conducted over 20 bidirectional cycles under 50% rated load. The gear ratio was measured as 6.5:1 with negligible deviation (<0.03%). The system showed stable performance, with a TE of $-0.34° \pm 0.40°$ and a root mean square of 0.52°. The peak-to-peak TE was 2.36°, establishing the cycle-0 reference. The mean motor current was 161.8 ± 28.5 mA. Most measurements (93.5%) remained within nominal conditions (Tier 0, within ±1°), while 6.5% exceeded the ±1° threshold (Tier 1). No higher-level failures were observed (Figure 4).

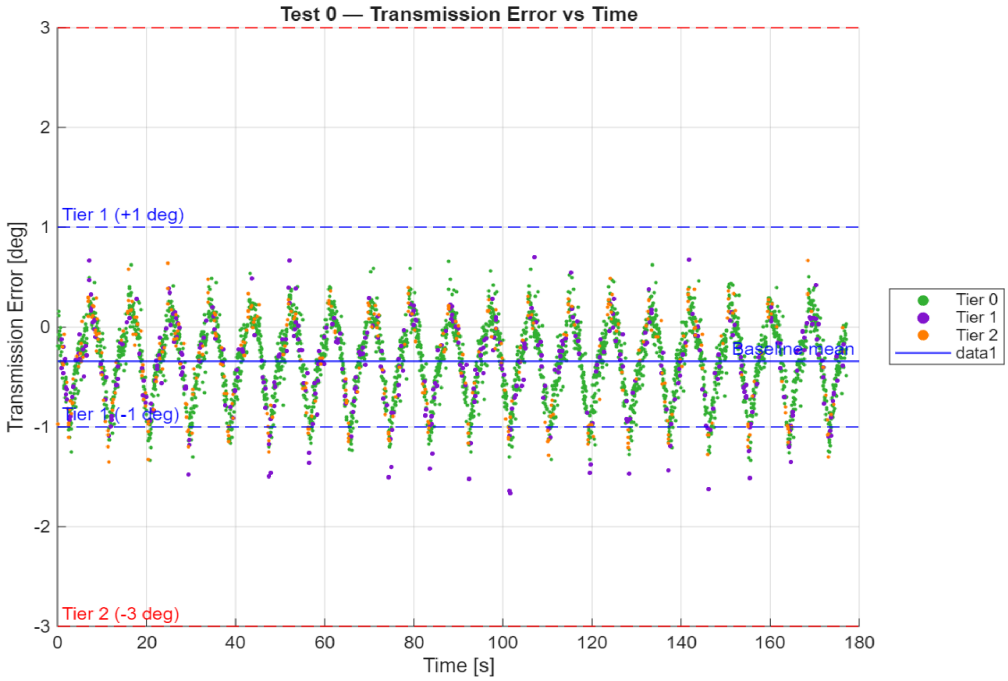

Figure 4. Baseline characterization: TE vs. time. Dashed blue and red lines mark the ±1° (Tier 1) and ±3° (Tier 2) thresholds; the solid line is the baseline mean.

The baseline transmission error shows a stable, periodic pattern across all 20 cycles with a systematic offset of −0.34°, consistent with rope elasticity under load. Peak errors at motion reversals occasionally exceed the ±1° Tier 1 threshold but remain well within the ±3° Tier 2 bound, confirming mechanical integrity and establishing a reliable cycle-0 reference for subsequent degradation analysis. The transmission error magnitude increased monotonically with applied load, from −0.52° at 0% to −1.47° at 80% rated torque. This corresponds to a sensitivity of approximately −0.0115° per % load. The relationship is nonlinear but is approximated linearly for practical purposes. All values remained within the ±3° threshold, indicating no intermediate failure under the tested loads. Repeatability improved at higher loads, with reduced variation between test passes. A consistent directional asymmetry (0.75°) was observed across all load levels, reinforcing the friction-dependent nature of the capstan mechanism (Table 3).

Table 3. Mean transmission error (TE) magnitude under incremental loading.

Applied Load %	Mean TE (°)
0 (Baseline)	0.51787
20	0.70749
40	0.91449
60	1.09964
80	1.46927

The creep test assessed positional drift under 50% rated torque over 30 min across three repetitions. Drift stabilized rapidly after initial settling, reaching a steady-state mean of 0.760° ± 0.052°, well within the ±1° minimal failure threshold, with no failure events recorded across any repetition (Table 4).

Table 4. Positional drift (creep) over 30 min under constant static load.

Elapsed Time (Min)	Rep 1 Drift (Deg)	Rep 2 Drift (Deg)	Rep 3 Drift (Deg)	Mean ± Standard Deviation (SD) (°)
1 (initial)	0.700	0.790	0.620	0.703 ± 0.085
5	0.790	0.700	0.790	0.760 ± 0.052
15	0.790	0.700	0.790	0.760 ± 0.052
30	0.790	0.700	0.790	0.760 ± 0.052

The endurance test consisted of three runs of continuous bidirectional cycles from 0° to 100° at constant speed under 55% rated load, accumulating 54,000 cycles in total (Table 5). In Run 1, the rope failed at 14,000 cycles by fatigue fracture of individual wires at the drum contact zone, which was classified as a critical failure (Table 2). Runs 2 and 3 each completed the 20,000-cycle test window without critical failure and were therefore treated as right-censored. The resulting Weibull parameters are summarized in Table 6.

Table 5. Cycles to failure and event categorization for Capstan Drive samples.

Test	Applied Load	Cycles to Failure (N_f)	Failure Mode (Categorized)	Cause
1	55%	14,000	Failure (Critical)	Rope wire fracture (fatigue)
2	55%	20,000	Censored (Right)	No failure (Survival test window)
3	55%	20,000	Censored (Right)	No failure (Survival test window)

Table 6. Weibull reliability parameters from endurance testing.

Parameter	Symbol	Value	Interpretation
Shape parameter	β	2.0	Assumed value for wire rope fatigue (wear-out).
Scale parameter	η	31,560 cycles	Maximum likelihood estimate of characteristic life; 90% lower confidence bound ≥ 20,798 cycles.
MTTF	$MTTF$	27,969 cycles	Expected mean life under 55% rated load.
Correlation	R^2	Not available	Not applicable for 1-parameter assumption (1 failure).

With one critical failure and two suspensions, the maximum likelihood estimate of the characteristic life is approximately 31,560 cycles, with a 90% lower confidence bound of 20,798 cycles and an MTTF of about 27,969 cycles (Table 6). For the reliability analysis using the Weibull distribution method, failures categorized as critical (Table 2) were defined as hard failures (end of life), whereas intermediate failures were treated as suspensions or soft failures in the statistical model (Table 7).

Table 7. Failure categorization for the Weibull Statistical Model.

Severity Level	Failure Criteria	Type of Failure
Critical	Structural breakage or TE $> 15°$	Hard failure (End of life)
Intermediate	Permanent slippage or TE $> \pm 3°$	Suspension/Soft failure
Minimal	Audible noise/Temperature increase	Operational Warning

4. Discussion and Conclusions

The results of this study confirm that capstan drives deliver low-backlash, smooth, and efficient transmission, making them suitable for precision applications. Their performance, however, is highly dependent on rope tension and friction conditions, with degradation over time caused by slip and elastic effects. Overall, capstan drives represent a viable option in applications requiring compliance and accuracy, but they demand careful control and maintenance to ensure reliable operation. The endurance testing program accumulated 54,000 cycles across three runs. A critical rope fatigue failure, characterized by fractured wires at the drum contact zone, occurred at 14,000 cycles in Run 1, while Runs 2 and 3 completed 20,000 cycles each without failure. A one-parameter Weibull analysis ($\beta = 2.0$ fixed, maximum likelihood estimation with suspensions) produced a characteristic life estimate of approximately 31,560 cycles and a conservative 90% lower confidence bound of at least 20,798 cycles, corresponding to a mean time to failure of about 27,969 cycles. These findings provide a statistically meaningful basis for assessing industrial feasibility.

The results also highlight the importance of the drum-to-rope diameter ratio in steel wire rope capstan drives. Early prototypes with undersized input drums failed prematurely due to excessive bending stress, whereas replacing them with geometrically appropriate drums significantly improved longevity, offering a concrete design guideline for practitioners. Furthermore, the observed failure mode—rope wire fracture without a preceding transmission error threshold crossing—demonstrates that visual inspection of the rope contact zone is a necessary complement to automated error monitoring in any reliable condition-monitoring strategy.

Limitations in this study must be acknowledged. The endurance runs were conducted on the same capstan drive assembly rather than independent units, meaning the Weibull estimate reflects rope life under specific mechanical conditions rather than population variability across manufactured systems. The shape parameter $\beta = 2.0$ was assumed from wire rope fatigue literature rather than estimated from a larger dataset. Future work should involve testing multiple independent rope installations across different units and higher cycle counts to enable full two-parameter Weibull estimation. Additionally, degradation analysis of transmission error progression or statistical process control of motor current drift could provide early warning of impending failure without requiring complete rope fracture, and these approaches should be explored in subsequent studies.

Author Contributions: Conceptualization, F.A. and S.-H.L.; methodology, F.A. and G.B.; investigation, F.A.; data curation, F.A.; formal analysis, G.B.; writing—original draft preparation, F.A. and G.B.; writing—review and editing, S.-H.L. and M.A.; supervision, S.-H.L. All authors have read and agreed to the published version of the manuscript.

Funding: This research was supported by the Intelligent Manufacturing Innovation Center (NTUST) within the Featured Areas Research Center Program and the Higher Education Sprout Project Framework of the Ministry of Education, Taiwan.

Institutional Review Board Statement: Not applicable.

Informed Consent Statement: Not applicable.

Data Availability Statement: The data presented in this study are available on request from the corresponding author.

Conflicts of Interest: The authors declare no conflicts of interest.

References

1. Thokale, M.J. Mechanical power amplifier working on a capstan principle. *IJARIIE* **2016**, *2*, 689–695.
2. Attaway, S.W. The mechanics of friction in rope rescue. In Proceedings of the International Technical Rescue Symposium (ITRS 99), Albuquerque, NM, USA, 5–7 November 1999.
3. Jung, J.H.; Pan, N.; Kang, T.J. Generalized capstan problem: Bending rigidity, nonlinear friction, and extensibility effect. *Tribol. Int.* **2008**, *41*, 524–534. [CrossRef]
4. Hwangbo, J.; Tsounis, V.; Kolvenbach, H.; Hutter, M. Cable-driven actuation for highly dynamic robotic systems. *arXiv* **2018**, arXiv:1806.10632.
5. Mazumdar, A.; Spencer, S.J.; Hobart, C.; Dabling, J.; Blada, T.; Dullea, K.; Kuehl, M.; Buerger, S.P. Synthetic fiber capstan drives for highly efficient, torque controlled, robotic applications. *IEEE Robot. Autom. Lett.* **2017**, *2*, 554–561. [CrossRef]
6. Tomaszewski, J. *Designing, Manufacturing and Testing Capstan Drive for Quadruped Robots*; Intermediate Project; Wrocław University of Science and Technology: Wrocław, Poland, 2022.
7. Lickindorf, D. *3-DoF Leg for a Quadruped Robot*; Intermediate Project; Wrocław University of Science and Technology: Wrocław, Poland, 2021.
8. Baser, O.; Konukseven, E.I. Theoretical and experimental determination of capstan drive slip error. *Mech. Mach. Theory* **2010**, *45*, 815–827. [CrossRef]
9. *IEC 60812:2018*; Failure Modes and Effects Analysis (FMEA and FMECA). International Electrotechnical Commission: Geneva, Switzerland, 2018.
10. Rinne, H. *The Weibull Distribution: A Handbook*; CRC Press: Boca Raton, FL, USA, 2008.
11. *ISO 9283:1998*; Manipulating Industrial Robots—Performance Criteria and Related Test Methods. International Organization for Standardization: Geneva, Switzerland, 1998.
12. Musa, A. Capstan-Drive: Robotic Actuator Test Stand Utilizing a Capstan Drive Reducer. GitHub, 2021. Available online: https://github.com/aaedmusa/Capstan-Drive (accessed on 19 April 2026).
13. Moradi, M.; Meiabadi, S.; Kaplan, A. Effect of 3D printing parameters on the fatigue properties of parts manufactured by fused filament fabrication: A review. *Appl. Sci.* **2023**, *13*, 904. [CrossRef]
14. Szykiedans, K.; Credo, W.; Osiński, D. Selected mechanical properties of PETG 3-D prints. *Procedia Eng.* **2017**, *177*, 455–461. [CrossRef]
15. ReliaSoft. Bayesian-Weibull Analysis. Available online: https://help.reliasoft.com/weibull20/bayesian_weibull_analysis.htm (accessed on 19 April 2026).

Disclaimer/Publisher's Note: The statements, opinions and data contained in all publications are solely those of the individual author(s) and contributor(s) and not of MDPI and/or the editor(s). MDPI and/or the editor(s) disclaim responsibility for any injury to people or property resulting from any ideas, methods, instructions or products referred to in the content.